JOURNAL OF APPLIED ELECTROCHEMISTRY **24** (1994) 719–724

Coplanar interdigitated band electrodes for electrosynthesis
Part II: Methoxylation of furan

C. BELMONT

University of Edinburgh, Chemistry Department, West Mains Road, Edinburgh EH9 3JJ, Great Britain

H. H. GIRAULT

Institut de Chimie Physique III, Ecole Polytechnique Fédérale de Lausanne, 1015 Lausanne, Switzerland

Received 1 September 1993; revised 24 November 1993

Four different platinum coplanar interdigitated band electrodes were screen printed on alumina and their roughness factors were determined by both electrochemical means and by scanning electron microscopy. The influence of the flow rate on the mass transport was investigated and compared with a classic parallel plate cell. The interdigitated printed electrodes were then used for the methoxylation of furan. It was shown that an excellent mass transport could be obtained in a tank reactor. Comparison with a pump cell or packed bed bipolar cell was made. When a 3 V potential difference was applied between an anode and a cathode separated by 250 μm, the current efficiency was 87% and the energy consumption was only 1.4 kW h kg^{-1}. Furthermore, the synthesis was found to be very selective, with only one major byproduct.

1. Introduction

Good mass transport conditions are of prime necessity for the success of many electrosyntheses. Although this is not a major problem if electrodes are widely spaced, it is still very important for an economic viewpoint to limit the interelectrode distances and thereby minimize the energy loss due to the Joule heating effect. For most conventional cells [1, 2], a decrease in the *iR* drop is associated with difficult mass transport or with an increase in the pumping cost. In a previous communication [3], a new type of electrolysis cell was proposed consisting of interdigitated planar band electrodes with submillimetre interelectrode spacing. These were fabricated by screen printing carbon or metallic inks. In particular, it was demonstrated that, compared to a parallel plate cell, the ohmic drop could be reduced by 50% without hindering hydrodynamics.

The behaviour of microband arrays is already thoroughly characterized for conducting sensors [4, 5] and also for amperometric detectors [6, 7]. Microelectrodes are of great interest in analytical chemistry because of their considerable sensitivity and their ability to work in resistive media [8–11]. The purpose of this work is to apply microelectrode technology to the fabrication of large scale electrodes with interelectrode distances of micrometres. Large scale arrays can be fabricated by screen printing. This technique constitutes a highly versatile means of producing electrodes at low cost. Of all the commercially available inks, a platinum paste is chosen for its specific electrochemical properties. The electrodes produced are porous and the currents observed are thus larger than those obtained with smooth surface electrodes. This type of electrode is investigated for the furan methoxylation which is a well documented electrosynthesis. Furan is oxidised to 2,5-dihydro 2,5-dimethoxy furan (DHDMF) which leads to very useful intermediates. The reaction is carried out in methanol via the *in situ* electrogeneration of bromine according to Scheme 1:

anode: $2Br^- \longrightarrow Br_2 + 2e^-$

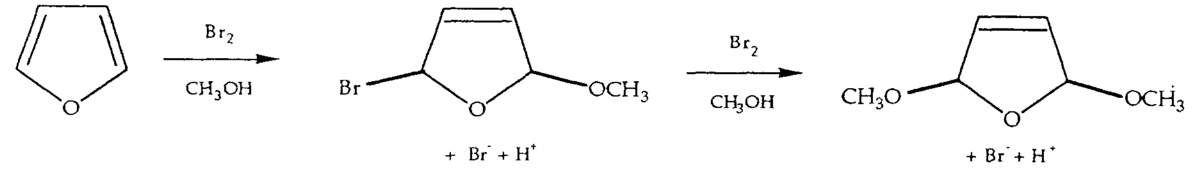

cathode: $2CH_3OH + 2e^- \longrightarrow H_2 + 2CH_3O^-$

Scheme 1.

0021-891X © 1994 Chapman & Hall

Table 1. Geometry of the interdigitated arrays

Array	*Total number of bands*	*Band gap* /mm	*Electrode width*/mm	*Band length* /mm
1	30	1 ± 0.1	1 ± 0.1	20 ± 1
2	40	0.5 ± 0.1	1 ± 0.1	20 ± 1
3	50	0.25 ± 0.05	1 ± 0.1	20 ± 1
4	70	0.25 ± 0.05	0.5 ± 0.1	20 ± 1

The identity of the intermediate is not certain but it is thought to react fast. DHDMF is sensitive to local acidic conditions. This reaction has been carried out in a large number of cells on graphite or platinum electrodes. Figures of merit can be found in the literature for pump cells [12–14], packed bed bipolar cells [15], tubular flow cells [16], perforated rotating electrodes [17] and also for the direct oxidation in an ion exchange membrane cell [18–20]. The current efficiency for a stirred tank reactor is the poorest and is about 10 times lower than for a pump cell or a packed bed bipolar cell where it reaches 80%. Jansson and Fleischmann [13] showed that good mass transport is essential for the selectivity of the synthesis. Best material yields (90%) have so far been obtained with packed bed bipolar cells for an energy consumption of 3 kW h kg^{-1}. The advantage of this type of cell design is the small interelectrode distances and thus the small ohmic loss. The disadvantages include current bypasses and a large dispersion in the hydrodynamic conditions, leading to several side reactions. As a result, as many as 11 byproducts can be detected with this cell. Mixing is more efficient in a pump cell, and the number of coproducts formed is reduced to four, but the pumping costs and the associated engineering difficulties can not be neglected.

2. Experimental details

Four different platinum arrays were printed on alumina (96%, Hederman & Porret, Switzerland) with a semi-automatic screen printer (DFS05, DickFilm System, Switzerland). Masks were designed with ordinary graphic software (Paintbrush on Microsoft Windows, US). The resolution was satisfactory for band gaps larger than 200 μm. Arrays were then printed on transparencies with a 300 dpi laser printer. For smaller dimensions, software originally developed for printed circuit boards combined with a laser photo-plotter should be used. The screens consisted of a 15 μm photosensitive film applied on stainless steel wires of 30 μm diameter and the mesh (number of wires per inch) was at 325 for the best definition. Four arrays were developed on the same screen. The platinum ink (JM 7601, Johnson Matthey & Brandberger AG, Switzerland) contained 83% of platinum and had to be cured at 900° C. Contacts were then isolated with fluorosilicone. Their geometrical descriptions can be found in Table 1. For a printed band electrode of 1 mm width, the resistance was found to be lower than 0.5 Ω cm^{-1}. 1 cm^2 square electrodes were also printed for surface characterization purposes.

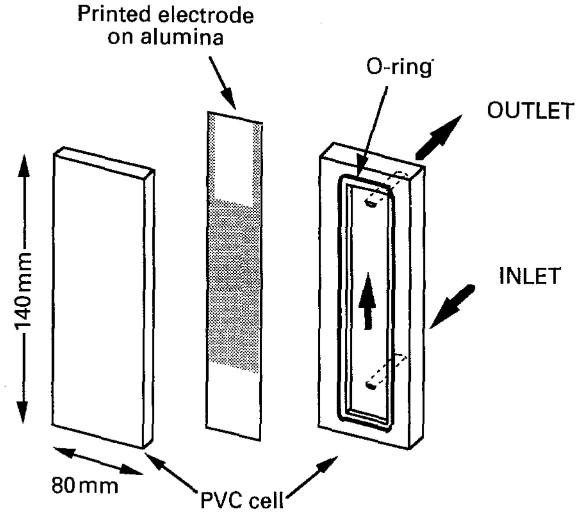

Fig. 1. Flow cell scheme.

The electrode surfaces were characterized by cyclic voltammetry of 1 cm^2 platinum electrodes in 1 M sulphuric acid, and by scanning electron microscopy (SEM) (Jeol, JSM 6300F). Cyclic voltammograms were recorded with a Sycopel ramp generator and potentiostat.

The influence of the flow rate on the mass transfer was investigated in a flow cell having a 4 mm × 20 mm internal cross section. This cell was placed in a flow loop of 250 ml total volume, where the flow rate was promoted with a pump (EMP40 Totton, UK). A scheme of this cell is shown in Fig. 1. The solution studied was a mixture of potassium ferricyanide (1 mM) and potassium ferrocyanide (1 mM) in 0.1 M NaCl.

Syntheses were carried out at 20° C in a cylindrical 150 ml stirred tank reactor represented in Fig. 2, and

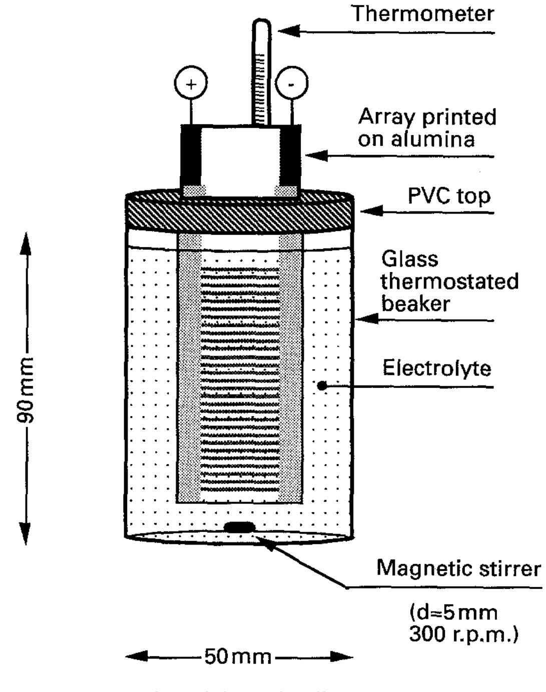

Fig. 2. Representation of the tank cell.

in the flow cell with flow rate set at 0.2 $\text{dm}^3\,\text{min}^{-1}$. The differential potential between the electrodes was applied with a PL320 QMD Thurlby constant voltage power generator in the range of 2.5 to 5 V and reversed every 2 min, using a home-made potential inverser. The amount of electricity passing through the cell was recorded continuously with a IG5N Tacussel integrator until complete consumption of the reactant. Furan and sodium bromide concentrations were kept, respectively, at 10% and 0.1 M for all the syntheses. The organic species present in the electrolyte were monitored progressively with a HP 5890 gas chromatograph equipped with a 20 m semi-capillary column filled with Carbowax 20 M. The temperature was programmed to stay at 60° C for 2 min before rising to 170° C at a rate of 30° C min^{-1}.

3. Results and discussion

3.1. *Surface characterization*

Cyclic voltammetry is a technique widely used for metal surface characterization [21, 22]. Platinum in an aqueous sulphuric acid solution, for example, shows typical adsorption and desorption peaks when the electrode potential is swept reversibly between 0 and 1.55 V vs NHE. Voltammograms recorded with a 1 cm^2 printed platinum electrode, before use and after 100 h of electrosynthesis showed the characteristic peaks resulting from hydrogen and oxygen reaction on the surface. Strongly and weakly adsorbed hydrogen oxidizes between 0 and 0.4 V vs NHE. The platinum surface is then bare and the non faradaic current is only due to the presence of a double layer. An oxide layer is formed between 0.8 and 1.5 V prior to oxygen evolution. On the reverse sweep the oxide is reduced at 0.7 V and the platinum surface is bare again until 0.4 V, where the two types of hydrogen start to adsorb. Assuming a monolayer coverage of adsorbed hydrogen, the areas of the desorption peaks correspond to the number of active sites on the electrode surface. A roughness factor is derived from the comparison of the electroactive and the apparent areas. Since platinum crystallizes in a cubic close packed structure, the amount of charge for a polycrystalline platinum surface can be averaged to 170 $\mu\text{C}\,\text{cm}^{-2}$. The integration of the hydrogen desorption peaks corresponds to 9.15 mC for the freshly printed platinum electrode. The roughness factor is thus evaluated at 54. Whereas after 100 h of electrosynthesis, the charge involved for the adsorbed hydrogen oxidation decreases to 6.64 mC, which corresponds to a roughness factor of 39. The electrodes appear to have been polished.

Scanning electron micogaphy was also used for surface electrode characterization. Scanning electron micrographs of the printed platinum electrodes at different stages confirmed the change in the surface roughness with electrosynthesis. The polishing effect of the synthesis is thus verified.

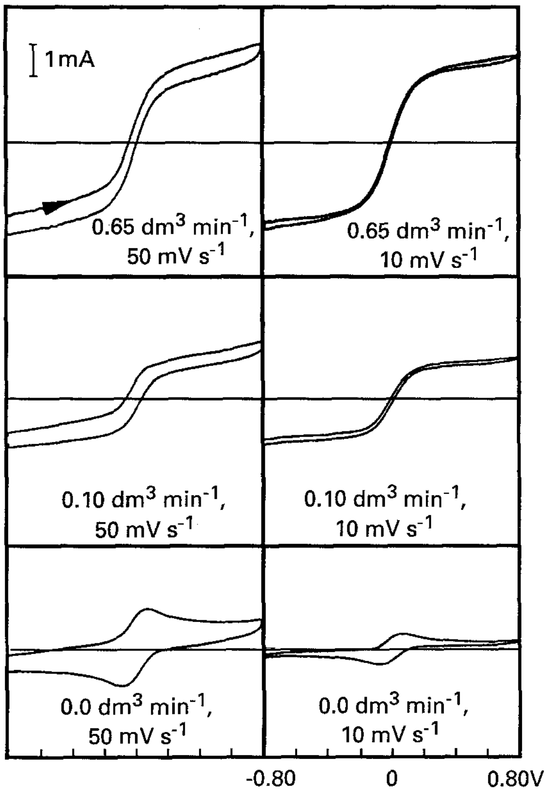

Fig. 3. Cyclic voltammograms recorded with interdigitated electrode array 2 in 1 mM potassium ferricyanide, 1 mM potassium ferrocyanide and 0.1 M NaCl aqueous solution. One electrode connected to the working electrode terminal, and the other connected to the reference and counter terminals of a potentiostat.

3.2. *Mass transfer characterization*

The mass transfer obtained with coplanar band electrodes is an essential parameter to investigate. Indeed the performance of a cell can be thoroughly characterized by the mass transfer coefficient, k_m, which is dependent on the fluid hydrodynamics and on the specific electrochemical properties of the compounds considered. k_m is usually determined from the limiting current for a given electrochemical process, but can also be calculated from the Sherwood number, which is related to three other dimensionless numbers:

$$k_\text{m} = \frac{I_\text{lim}}{nFAc} = \frac{D}{L}Sh = \frac{D}{L}aRe^bSc^cGr^d \qquad (1)$$

Where I_lim is the limiting current, n the number of electrons involved in the reaction, F the Faraday constant, c the concentration of the electroactive species, D the diffusion coefficient, L the equivalent diameter of the cell, Sh the Sherwood number, Re the Reynolds number, Sc the Schmidt number, Gr the Grashof number, and finally a, b, c and d four coefficients.

For a given electrochemical process, the flow rate has a fundamental influence on the mass transfer coefficient. Figure 3 shows the cyclic voltammograms recorded by applying a differential potential between the anode and the cathode of a platinum interdigitated array 2, in a solution containing Fe(CN)_6^{3-} and Fe(CN)_6^{4-} ions. A steady state response is observed when the electrolyte is forced to flow through the cell, and the scan rate is found to have

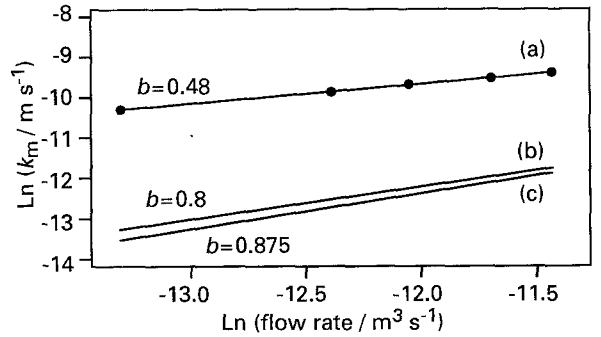

Fig. 4. Evolution of the mass transfer with the flow rate, when k_m is determined: (a) experimentally with the coplanar interdigitated band electrodes from array 2, (b) from Equation 3 and (c) from Equation 4.

no effect on the current amplitude for a given flow rate. From this figure it can also be verified that the mass transfer, and thus the limiting currents, associated with the reduction or the oxidation of these ions, decrease significantly with the flow rate. From Equation 1, it can be demonstrated that the mass transfer coefficient is logarithmically proportional to the flow rate:

$$\ln k_m = k_0 + b \ln(\text{flow}) \tag{2}$$

With the platinum array 2, the values of k_0 and b were respectively −3.89 and 0.48. Changing the band gap had very little effect on the mass transfer and the value of the coefficient did not vary in a great extent.

For a classical two parallel plate cell, the values of the coefficient a, b, c, and d introduced in Equation 1, can be found in the literature. The expressions given by Cœuret and Stork [23], and by Pickett and Stanmore [24], Equations 3 and 4, are developed for turbulent regimes, and thus already overestimate the mass transfer in a laminar flow cell.

$$Sh = 0.023\, Re^{0.8} Sc^{0.33} \tag{3}$$

$$Sh = 0.0278\, Re^{0.875} Sc^{0.21} \tag{4}$$

Figure 4 shows a comparison of the mass transfer coefficient determined experimentally with array 2 and the mass transfer coefficients that would be obtained with two parallel plate electrodes under the same conditions, calculated from Equations 3 and 4. The linear relationship proposed in Equation 2 is verified and the mass transfer is found to be considerably improved by using coplanar band electrodes. Furthermore, the flow between two parallel plate electrodes must be increased to 0.6 dm^3 min^{-1} before it reaches the value obtained with the coplanar array at zero flow. This important characteristic implies that this electrode geometry could have interesting applications in tank reactors, with low convection regimes.

Table 2. Figures of merit for different experimental conditions

Array	Flow /dm^3 min^{-1}	Applied voltage /V	Current densities /A dm^{-2}	Material yield /%	Current efficiency /%	Energy consumption /kW h kg^{-1}
1	–	3	4.7	46	61	2.0
2	0.2	2.5	3.5	33	68	1.5
2	0.2	3	6.2	57	75	1.6
2	0.2	5	18.7	76	70	2.9
2	–	3	5	63	83	1.4
2	–	5	15	75	67	3.1
3	–	3	14	78	87	1.4
4	–	3	8.5	53	75	1.6

3.3. *Furan methoxylation*

From all the experiments carried out, it should be stressed that traces of several byproducts are detected, but effectively only one major coproduct is affecting the yields. High current densities are recorded. They are found to be constant with time and vary in the range 3.5 to 18.7 A dm^{-2}, depending on the experimental conditions. Figures of merit are necessary to show the influence of parameters such as the convection, the applied voltage and the array geometry. Current efficiencies and energy consumptions are very stable with time. Their values for different experimental conditions can be found in Table 2, where material yields and current densities are also reported.

3.3.1. Convection. For this electrochemical process, the dominant mass transport regimes are convection and diffusion. In the flow cell, with flow rate set at 0.2 dm^3 min^{-1}, the Reynolds number is low

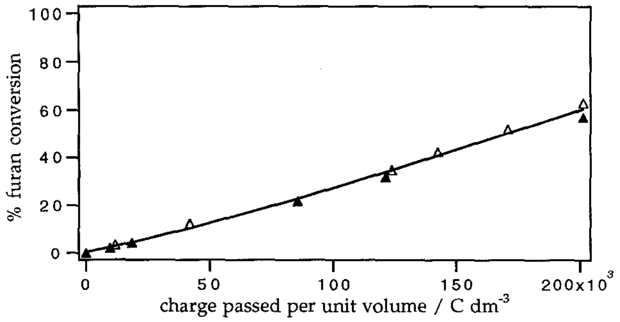

Fig. 5. Evolution of the conversion of furan into DHDMF with the normalized amount of electricity used, for two cell configurations, array 2 at 3 V. (▲) Flow cell and (△) tank cell.

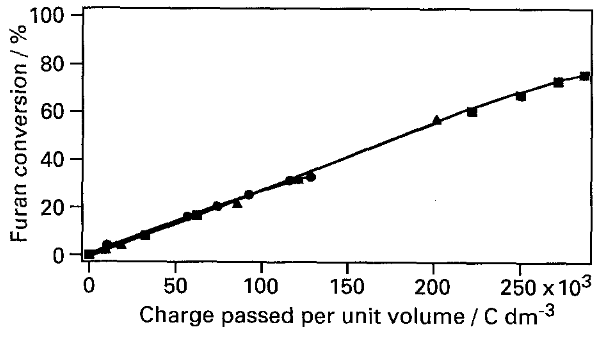

Fig. 6. Evolution of the conversion of furan into DHDMF, with the normalized amount of electricity used, for different applied voltage and with array 2 in the flow cell. (●) 2.5 V, (▲) 3 V and (■) 5 V.

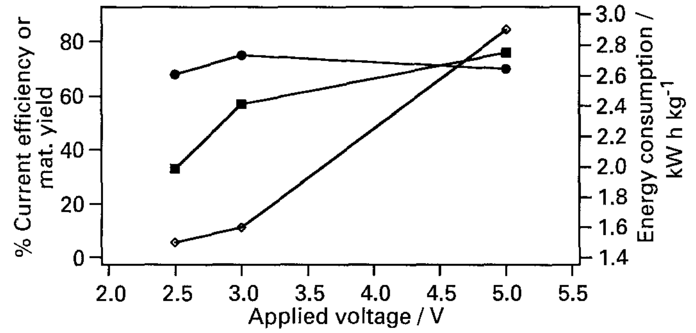

Fig. 7. Effect of the applied voltage on the three figures of merit. (■) Material yield, (●) current efficiency and (◇) energy consumption.

($Re \simeq 300$) and convection is purely laminar. The convection in the tank is, however, more complex as it is due to the combination of random magnetic stirred agitation and gas evolution. Hydrogen formed at the cathodes rises vertically against the array, thus producing a micro flow. It can be seen in Fig. 5, that with both tank cell and flow cell, the conversion of furan into DHDMF increases very regularly with the amount of charge passed through the cell, to reach comparable values. Furthermore, the experiments carried out in the tank reactor and in the flow cell with array 2 show that the flow conditions have little effect on current efficiency and energy consumption. This characteristic was observed when the potential was set at 3 V, as well as at 5 V. This is extremely interesting as it implies that, under these conditions, the mass transport is not affected by the flow. Syntheses can thus be performed in a tank reactor instead of flow cells, suppressing pumping cost and removing all the problems associated with complicated installations.

3.3.2. Applied voltage. Figure 6 represents the increase of the conversion of furan into DHDMF with the normalized amount of charge passed through the cell, for electrosyntheses carried out in the flow cell with array 2, at three different potentials. As in Fig. 5, a very good correlation exists for the three applied voltages. However, it should be noticed that the electrosynthesis time and the material yield are particularly affected by the value of the applied voltage. The material yield for example varies from 33 to 76% when the potential is increased from 2.5 to 5 V, and the electrosynthesis time is reduced from 50 to 26 h. The values of the current efficiency and the energy consumption are reported in Fig. 7. The current yield is affected by the applied voltage to a lesser extent. It varies in the range 68 to 75%, the optimum value being obtained at 3 V. The experiments carried out by M. J. Medeiros *et al.* [25] on platinum microdisc electrodes showed that a very steady-state plateau can be obtained from the sodium bromide oxidation in methanol. However, the bromide oxidation potential for the platinum arrays is difficult to determine with accuracy as the solvent electrolysis occur simultaneously. It can, however, also be estimated to be around 3 V. The energy consumption also varies with the applied potential. Its value almost doubles from 1.6 to 2.9 kW h kg^{-1}, when the voltage is increased from 3 to 5 V. It is thus more advantageous to carry out the synthesis at low voltage. The choice of the optimum applied voltage thus results from a compromise and can be set at 3 V.

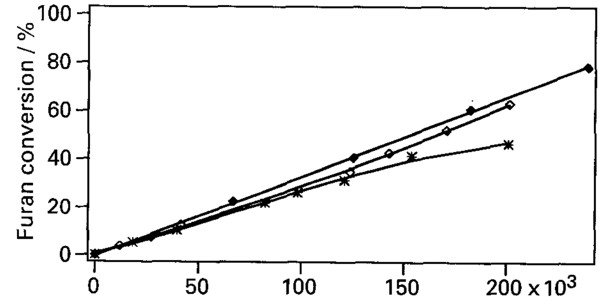

Fig. 8. Evolution of the conversion of furan into DHDMF with the normalized amount of electricity used, for three different arrays in the tank cell at 3 V. (*) 1 mm band gap, (◇) 0.5 mm band gap and (◆) 0.25 mm band gap.

3.3.3. Array geometry. The advantage of having small interelectrode distances is illustrated by performing electrosynthesis in the tank reactor on arrays with 1 mm bandwidth electrodes and interelectrode distances varying in the range 1 mm to 250 μm. Figure 8 shows the evolution of the furan conversion into DHDMF for the three different arrays, as the normalized amount of electricity passed through the array is increased. Reducing the interelectrode distance has the effect of increasing the material yield. This is an interesting aspect and a possible explanation of such a phenomena is the neutralization of the protons, responsible for the DHDMF degradation, by the methanolic ions produced at the adjacent band electrode. The effect of decreasing the band gap is also illustrated in Fig. 9, where the three figures of merit are reported. Similarly, the current efficiency is increased by decreasing the band gap and reaches a value of 87% for a 250 μm gap. The energy consumption decreases with the band gap but stabilizes at 1.4 kW h kg^{-1} below 500 μm, although this value is higher than the value estimated thermodynamically (0.6 kW h kg^{-1}).

Table 3. Figures of merit for different cells

Figures of merit	*Array 3*	*Packed bed bipolar cell*
Material yield/%	78	90
Current efficiency/%	87	90
Energy consumption/kW h kg^{-1}	1.4	3

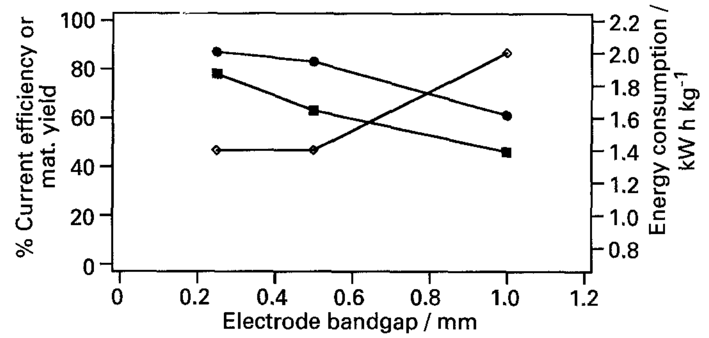

Fig. 9. Effect of the band gap on the three figures of merit. (■) Material yield, (●) current efficiency and (◇) energy consumption.

Finally, the results obtained with array 4 show that reducing the band width from 1 to 0.5 mm worsens the performance of the array. However, without more data it is not possible to suggest an optimum bandwidth.

3.3.4. Optimal experimental conditions. From all the experiments carried out, it appears that the optimal experimental conditions are reached in the tank cell reactor, with the smallest electrode band gap and when the potential is set at 3 V. Figures of merit obtained with the 250 μm gap array in the tank cell are reported in Table 3 and compared with the performance of a bipolar packed bed cell. Figures compare extremely well, and in particular the energy consumption is decreased by a factor of 2.

4. Conclusion

This work shows that long-life platinum interdigitated band electrodes can be obtained by screen printing and that their application in electrosynthesis is very advantageous. Their porosity, characterized by electrochemical means, implies that their active surface is 54 times bigger than their geometrical area. Excellent mass transfer conditions are observed and application to the furan methoxylation proves that this new type of electrode is able to seriously compete with the packed bed bipolar cell, considered so far to be the most efficient cell. Hydrogen formed on the cathode rises along the array and provides a satisfactory mixing. The reaction can thus be carried out in a tank cell rather than in a flow cell. Hence, the cost of pumping and related equipment does not interfere in the total cost estimation of the cell. Furthermore, when the performance of a 250 μm band gap array in a tank cell, with the applied voltage set at 3 V, is compared to the bipolar packed bed cell, material yield is slightly less but could be improved by increasing the electrode area with respect to the cell volume to limit the time of reaction and thus furan evaporation. The current efficiency is very comparable, and the energy consumption is decreased from 3.0 to 1.4 kW h kg^{-1}, which results in a 50% gain. Electrosynthesis on interdigitated electrodes is thus a very economical process. To follow this investigation, a scale up will be considered, as well as syntheses with coupled reactions or reactions in very resistive media.

Acknowledgements

The authors thank Electricité de France Direction des Recherches who financed the project and also the Ecole Polytechnique Fédérale de Lausanne where all the experimental work was done. Finally, they are grateful to Dr C. Comninellis for helpful scientific discussions.

References

[1] D. Pletcher and F. C. Walsh, 'Industrial Electrochemistry', Chapman & Hall, London, (1990).

[2] F. C. Walsh, 'A First Course In Electrochemical Engineering', The Electrochemical Consultancy, Alresford Press (1993).

[3] C. Belmont and H. H. Girault, *J. Appl. Electrochem.*, in press.

[4] K. R. Wehmeyer, M. R. Deakin and R. M. Wightman, *Anal. Chem.* **57** (1985) 1913.

[5] A. J. Bard, J. A. Crayston, G. P. Kittelsen, T. V. Shea and M. S. Wrighton, *ibid.* **58** (1986) 2321.

[6] K. Aoki, K. Tokuda and H. Matsuda, *J. Electroanal. Chem.* **217** (1987) 33.

[7] J. L. Anderson, K. K. Whiten, J. D. Brewster, T. Y. Ou and W. K. Nonidez, *Anal. Chem.* **57** (1985) 1366.

[8] R. M. Wightman, *Anal. Chem.* **53** (1981) 1125R.

[9] M. I. Montenegro, M. A. Queiros and J. L. Daschbar (Eds.), 'Microelectrodes: Theory and Applications', NATO ASI series, **197** (1991).

[10] R. M. Wightman and D. O. Wipf, *Electroanal. Chem.* **15** (1989) 267.

[11] M. Fleischman, S. Pons, D. R. Rolison and P. P. Schmidt, 'Ultramicroelectrodes', Datatech Systems, Morganton, NC (1987).

[12] R. E. W. Jansson and N. Tomov, *Chem Ind. (London)* **3** (1978) 96.

[13] R. E. W. Jansson and M. Fleischmann, *AIChE Symp. Ser.* **185** (1979) 2.

[14] N. R. Tomov and R. E. W. Jansson, *J. Chem. Techn. Biotechnol.* **30** (1980) 110.

[15] K. Kusakabe, S. Morooka and Y. Kato, *J. Chem. Eng. Jpn.* **19** (1986) 43.

[16] A. J. Bellamy and B. R. Simpson, *Chem Ind. (London)* **21** (1982) 863.

[17] V. Krishnan, A. Muthukumaran and H. V. K. Udupa, *Trans. SAEST* **14** (1979) 39.

[18] E. Raoult, J. Sarrazin and A. Tallec, *J. Appl. Electrochem.* **15** (1985) 85.

[19] K. H. Simmrock, R. Gregel, R. Fabiunke, J. Jörissen and Köhler, *Proc. Electrochem. Soc.* **88** (1988) 383.

[20] C. Moinet, J. Sarrazin and A. Tallec, *Bull. Soc. Chim. Fr.* **1** (1983) 184.

[21] Y. Duhirel, B. Beden, J. M. Léger and C. Lamy, *Electrochim. Acta* **37** (1992) 665.

[22] A. Papoutsis, J. M. Léger and C. Lamy, *J. Electroanal. Chem.* **234** (1987) 315.

[23] F. Cœuret and A. Storck, Eléments de génie électrochimique, Technique et Documentation (1984).

[24] D. J. Pickett and B. R. Stanmore, *J. Appl. Electrochem.* **2** (1972) 151.

[25] M. J. Medeiros, M. I. Montenegro and D. Pletcher, *J. Electroanal. Chem.* **290** (1990) 155.